Neurosci. Bull. August, 2019, 35(4):697–708
https://doi.org/10.1007/s12264-019-00365-w

www.neurosci.cn
www.springer.com/12264

ORIGINAL ARTICLE

Medial Preoptic Area Modulates Courtship Ultrasonic Vocalization in Adult Male Mice

Shu-Chen Gao[1,2] · Yi-Chao Wei[1,2] · Shao-Ran Wang[1,2] · Xiao-Hong Xu[1]

Received: 28 August 2018 / Accepted: 11 October 2018 / Published online: 21 March 2019

Abstract Adult male mice emit highly complex ultrasonic vocalizations (USVs) in response to female conspecifics. Such USVs, thought to facilitate courtship behaviors, are routinely measured as a behavioral index in mouse models of neurodevelopmental and psychiatric disorders such as autism. While the regulation of USVs by genetic factors has been extensively characterized, the neural mechanisms that control USV production remain largely unknown. Here, we report that optogenetic activation of the medial preoptic area (mPOA) elicited the production of USVs that were acoustically similar to courtship USVs in adult mice. Moreover, mPOA vesicular GABA transporter-positive (Vgat +) neurons were more effective at driving USV production than vesicular glutamate transporter 2-positive neurons. Furthermore, ablation of mPOA Vgat+ neurons resulted in altered spectral features and syllable usage of USVs in targeted males. Together, these results demonstrate that the mPOA plays a crucial role in modulating courtship USVs and this may serve as an entry point for future dissection of the neural circuitry underlying USV production.

✉ Yi-Chao Wei
ycwei@stanford.edu

✉ Shao-Ran Wang
srwang@ion.ac.cn

✉ Xiao-Hong Xu
xiaohong.xu@ion.ac.cn

[1] Institute of Neuroscience, State Key Laboratory of Neuroscience, CAS Center for Excellence in Brain Science and Intelligence Technology, Chinese Academy of Sciences, Shanghai 200031, China

[2] University of the Chinese Academy of Sciences, Beijing 100049, China

Keywords mPOA · Optogenetics · Vgat · Vglut2 · Ultrasonic vocalization · Courtship

Introduction

Vocal communication is an important way for individuals of social species, ranging from humans and dolphins to bats, to convey information to other conspecifics in order to coordinate behaviors. At sexual maturity, male mice begin to emit ultrasonic vocalizations (USVs) in the presence of females or their pheromone cues but rarely do so towards other males [1–6], suggesting a role for USVs in male courtship behaviors. These USVs consist of distinct syllables organized in sequences and motifs in a song-like structure, which when pitch-drop to an audible frequency range sound like courtship songs in birds [7]. Functionally, female mice prefer vocalizing over non-vocalizing males [8], and more frequently approach empty chambers that play male USVs [9, 10], especially those with more complex patterns [11]. Furthermore, exposure to male USVs stimulates kisspeptin neurons in females and promotes their fertility [12].

Interestingly, female mice also vocalize towards other females [13], and the calling rate and acoustic features of such vocalizations are comparable to those produced by males [14]. In addition, a recent study showed that female mice also produce temporally coordinated USVs along with males during courtship chases, albeit much less often than males [15]. The functional relevance of these female-emitted USVs remains to be determined, but it is clear that female mice do have the capacity to produce USVs just like males.

In genetically or surgically-produced deaf mice, USVs occur and are mostly normal [16–18], suggesting that the

neural mechanisms underlying mouse USV production are innate. Consistent with this, variations in genetic background as well as mutations in single genes have been shown to greatly influence aspects of mouse USVs such as syllable repertoire, syntax, calling rate, and frequency [2, 19–25]. In particular, mice bearing deletions or mutations in candidate genes (for example, *Shank3*, *FoxP2*, *Neuroligin-3* and *-4*) that are linked to human diseases associated with communication deficits also show defects in USV production [26–30], suggesting conserved genetic codes. Because of this, USVs are routinely measured as a behavioral index in mouse models of neurodevelopmental and psychiatric disorders such as autism [31–33]. Furthermore, as the contents of mouse USVs are altered in a context- and experience-dependent manner, which demonstrates an ability for vocal modification [11, 16, 34–40], dissecting the neural mechanisms governing USV production in mice may provide insights into the neural control of vocal production in mammals in general [16, 41, 42].

Despite extensive studies on the regulation of USVs by genetic factors, sensory cues, and social experience/status, to date, the neural mechanisms that control USV production remain largely unknown. Given the connection between USVs and courtship, we hypothesized that brain areas critical for sexual behaviors may also regulate USV production in mice. Previously, we showed that optogenetic activation of the medial preoptic area (mPOA) drives male-typical sexual behaviors [43]. Here, we show that mPOA activation, in particular activation of neurons positive for the vesicular GABA transporter (Vgat), also promotes, in the absence of any social stimulus, the production of USVs that are acoustically similar to those emitted spontaneously by adult males towards a female. Furthermore, ablation of mPOA Vgat+ neurons, while not affecting gross USV levels, resulted in altered spectral features and syllable usage by targeted males. Together, these results provide an entry point for future investigation of the neural circuitry underlying USV production.

Materials and Methods

Animals

C57BL/6 J mice were purchased from The Jackson Laboratory (Bar Harbor, ME) and Shanghai Laboratory Animal Center (Shanghai, China) and bred in-house. Vglut2-Ires-Cre (Vglut2, vesicular glutamate transporter 2) (STOCK Slc17a6tm2(cre)Lowl/J) mice were purchased from The Jackson Laboratory. Vgat-Cre mice had been previously generated [44]. All Cre lines were bred onto the C57BL/6 J background for at least one generation. The mice were housed in the Institute of Neuroscience animal facility under a 12 h:12 h light/dark cycle with food and water *ad libitum*. Only animals heterozygous for Cre alleles were used. All experimental protocols were approved by the Animal Care and Use Committee of the Institute of Neuroscience, Chinese Academy of Sciences, Shanghai, China (IACUC No. NA-016-2016). Animals reported in this study partially overlapped with those in our previous study [43].

Surgery

Adult mice of 2 months–4 months old were anesthetized with isoflurane (0.8%–5%) and placed in a stereotactic frame (Model 1900, David Kopf Instruments, Tujunga, CA). Ophthalmic ointment was applied to prevent dehydration. The skull was exposed with a small incision and holes were drilled to inject virus through glass pipettes (15 μm–25 μm tip diameter) and to implant optical fibers. The coordinates for viral delivery into the mPOA were: AP, − 0.16 mm; ML, ± 0.4 mm; DV, − 5.15 mm (Paxios and Franklin Mouse Brain Atlas, 2nd edition). Virus was injected (100 nL per side–400 nL per side) at a flow rate of 70 nL/min using a home-made nanoliter injector or at 40 nL/min using a hydraulic pump (Harvard Apparatus, Holliston, MA). The pipettes were left in place for ∼ 10 min before retraction. Optical fibers (diameter, 200 μm; numerical aperture, 0.37; length, 6 mm; AniLab Software and Instruments Co., Ltd, Ningbo, China) were placed 400 μm above the virus injection site for optogenetic experiments. Optical fibers were secured with dental cement and skull screws. Littermates were randomly chosen to be injected with experimental or control virus. Animals were allowed 3 weeks–4 weeks to recover from surgery before behavioral tests.

Virus

The following viruses were used: AAVs-hSyn-ChR2-mCherry (Serotype 2/8, titer 2.26×10^{13} genomic copies/mL), AAVs-hSyn-mCherry (Serotype 2/8, titer 3.38×10^{12} genomic copies/mL), AAVs-Ef1a-DIO-ChR2-mCherry (Serotype 2/8, titer 7.39×10^{12} genomic copies/mL), and AAVs-Ef1a-DIO-mCherry (Serotype 2/8, titer 8.93×10^{12} genomic copies/mL), all of which were from Obio Technology Co. (Shanghai, China); AAVs-Ef1a-DIO-EYFP (Serotype 2/9, titer 8.6×10^{12} genomic copies/mL) was from Shanghai Taitool Bioscience Co., Ltd (Shanghai, China); and AAVs-Ef1a-DIO-taCasp3.Tevp (Serotype 2/5, titer 4.2×10^{12} genomic copies/mL) was from the University of North Carolina Gene Therapy Center Vector Core.

Behavioral Assays

The animals used for optogenetic activation were group-housed. On the day of the behavioral test, they were introduced to a fresh cage. An external optical fiber was used to connect a 473-nm laser power source (Shanghai Laser and Optics Century Co. or Changchun New Industries Optoelectronics Tech Co., Ltd.) to the implanted optical fiber in the animal. The external optical fiber was attached to a rotary joint (FRJ_1X1_FC_FC, Doric Lenses, Inc., Quebec, Canada) to allow the animal to freely behave. The tested animal was allowed to explore the cage for $\sim$ 15 min with the external fiber attached. Then, a custom MatLab program was started to control a Master-9 stimulator (AMPI, Jerusalem, Israel), which sent a trigger to initiate recording by the camera and sent commands to the laser to deliver 15 s of photostimulation (40 Hz, 12 mW), randomly spaced 90 s–120 s apart. The laser power was adjusted for each animal according to the luminance transitivity efficiency of the implanted optical fiber measured prior to implantation to assure that the power of the light emitted at the tip of the fiber was constant across animals. Five to 12 stimulations (15 s each) were delivered during each assay. During videotaping, sounds in the frequency range from 0 Hz to 125 kHz were recorded with a microphone and amplifier (UltraSoundGate, Avisoft Bioacoustics, Glienicke/Nordbahn, Germany) and digitized at 250 kHz and 16 bits. At the beginning of the test, the experimenter snapped his/her fingers in the video field to make an audible noise. This event was used later to synchronize the video and audio files. After all behavioral testing, *post-hoc* analysis of the targeting site was carried out as previously described [43]. To record spontaneously-emitted USVs, an animal housed singly for 1 weeks–3 weeks was video-taped with an infrared camera. After 5 min–10 min of adaptation, a hormone-primed female was introduced into the cage to freely interact with the experimental animal for $\sim$ 5 min. During the process, sounds in the frequency range from 0 Hz to 125 kHz were recorded with the microphone and amplifier (UltraSoundGate) and digitized at 250 kHz and 16 bits. Afterwards, male behaviors towards females were scored and aligned to USVs to separate those emitted during different stages of mating.

Analysis of Ultrasound

To analyze the levels of USV production, the stored waveforms in the recorded audio files were first converted to spectrograms using a short-time Fourier transform function (spectrogram.m) with a program custom-written in MatLab (128 samples/blockform, 0.2 ms temporal resolution, and 0.98 Hz frequency). With this program, USVs were automatically detected by the criterion of > 2 standard deviations above the baseline level and an area of the spectrogram > 15 pixels and frequencies > 30 kHz. Detected USVs with duration < 0.08 ms were recognized as noise and removed. All other extracted USVs were checked manually for accuracy. For optogenetic experiments, the finger-snap at the beginning of each video was automatically detected by the program by its high power across nearly all frequencies and was used to align the extracted USVs with the optogenetic stimulation periods to calculate the probability of USV occurrence and the onset latency of evoked USVs. Given the low background, USVs that occurred from the onset of light to within 15 s of light termination were all considered to be optogenetically activated. USVs that occurred after the termination of light stimulation had onset latencies > 15 s.

More detailed analysis of the spectral attributes and syllable composition of USVs was carried out in Mouse Song Analyzer v1.3 as previously described [7, 11, 16, 45, 46] with the "split s" box checked. Briefly, the software computed the sonograms from each waveform (256 samples/block, half overlap). We used a criterion of 3 ms as the minimum duration for syllable detection and a silence gap > 10 ms to separate two syllables. The identified syllables were then classified by the presence or absence of instantaneous "pitch jumps" and by the duration and trajectory of the pitch frequency. In all, 9 types were classified, 6 for syllables without any pitch jumps including "short", "flat", "upward (up)", "downward (down)", "chevron (chev)", and all others as "unclassified simple (us)", and 3 types for syllables with pitch jumps including those containing two notes separated by a single upward (type "u") or downward (type "d") pitch jump and more complex syllables containing two or more multiple pitch jumps (type "m"). Any sound that the software could not classify was removed from the analysis, most of which contained mechanic noises occurring during recordings. Files with persistent background noises throughout the recording session or < 100 syllables detected were also excluded from analysis and were not included in the plots. The identified syllables were quantified automatically by Mouse Song Analyzer v1.3 for the spectral parameters including syllable duration, inter-syllable interval, bandwidth, pitch (mean frequency), and spectral purity. Spectral purity was calculated as the instantaneous maximum power at the peak frequency normalized by the instantaneous total power in the spectrum, averaged across the entire syllable. A pure tone has a spectral purity of 1 and white noise approaches 0. For analysis of sequence length, a sequence was defined by a series of syllables that were > 250 ms apart from any other syllables. For spectral features, all syllables were grouped together for analysis. To calculate syllable composition, the

number of a particular syllable type was divided by the total number of syllables detected in each individual animal and then averaged across animals within each experimental group.

In Situ Hybridization

DNA templates for generating *in situ* probes were cloned using the following primer sets: *Vgat*, 5′-GCCATTCA GGGCATGTTC-3′ and 5′-AGCAGCGTGAAGACCACC-3′; *Vglut2*, 5′-ATCGACTAGTCCAAATCTTACGGTGCTAC CTC-3′ and 5′-ATCGCTCGAGTAGCCATCTTTCCTGT TCCACT-3′; and *GAD1* (glutamate decarboxylase 1), 5′-C ATTGAGGAGATAGAGAGGTTG-3′ and 5′-AGAGAAG AGCGAAGGCTACT-3′. Anti-sense RNA probes were transcribed with T7 RNA polymerase (Cat# P207E, Promega, Madison, WI) and digoxigenin-labeled nucleotides. Mice were anesthetized with 10% chloral hydrate and transcardially perfused with diethyl pyrocarbonate-treated PBS (D-PBS) followed by ice-cold 4% paraformaldehyde in D-PBS. Afterward, brains were cut at 40 μm on a vibratome (VT1000S, Leica, Nussloch, Germany). Brain sections were washed in 2 × SSC buffer containing 0.5% Triton for 30 min, acetylated in 0.1 mol/L triethanolamine (pH 8.0) with 0.25% acetic anhydride (*v*/*v*) for 10 min, equilibrated in pre-hybridization solution for 2 h at 65 °C and subsequently incubated with 0.5 μg/mL of specific RNA probes in hybridization buffer overnight at 65 °C. The next day, the sections were rinsed in pre-hybridization solution and Pre-Hyb/TBST (TBS with 0.1% Tween-20) for 30 min each. Next, the sections were washed twice with TBST and three times with TAE (Tris-acetate-EDTA) buffer, each for 5 min. Sections were then transferred to wells in 2% agarose gel, and run in 1 × TAE at 60 V for 2 h to remove unhybridized probes. The sections were then washed twice in TBST, and subsequently incubated with sheep anti-digoxigenin-Alkaline phosphatase (AP) (1:2000, Cat# 11093274910, Roche, Boston, MA), sometimes together with chicken anti-GFP antibody (1:300, Cat# ab13970, Abcam, Cambridge, MA) for co-staining purposes, in 0.5% blocking reagent (11096176001, Roche) at 4 °C overnight. On the next day, for bright-field staining, sections were washed and stained with 4-Nitro blue tetrazolium choloride (Cat# 11383213001, Roche) and 5-Bromo-4-chloro-3'-indolyl phosphate (Cat# 11383221001, Roche) for 4 h–10 h at 37 °C. For fluorescent *in situ* hybridization combined with immunohistochemistry, sections were first stained with fluorescent secondary antibodies, followed by staining with fast red (HNPP Fluorescent Detection Set, Cat# 11758888001, Roche) and counterstaining with DAPI (5 mg/mL, 1:1000, Sigma, St Louis, MO) in PBS. All sections were washed after staining and mounted on glass slides. Images were captured with a 20 × objective on a conventional or confocal microscope. Images were processed and counted in ImageJ (NIH). All counting was done by experimenters blind to the sex and the test condition of the animal. An area in the center of the injection site was selected from each animal to analyze the co-labeling of EYFP and *Vglut2* or *Vgat*.

Statistical Analysis

In bar graphs, data are presented as mean ± SEM. In box and whiskers plots, data are presented as min to max whiskers, the mean is indicated by "+", and the median indicated by a horizontal line. Data with two independent variables were analyzed by two-way ANOVA followed by a *post hoc* test with Bonferroni correction. For comparison of two groups, if the variances were tested to be equal with the function vartest2 (MatLab, Natick, MA) and the data were tested for a Gaussian distribution with lillietest in MatLab, *P* values were calculated with two-tailed Student's *t*-test; otherwise, they were calculated with the Wilcoxon signed rank test for matched pairs and the Wilcoxon rank sum test for non-paired tests. Categorical data were compared with Fisher's exact test. $*P < 0.05$, $**P < 0.01$, $***P < 0.001$.

Results

Optogenetic Activation of the mPOA Elicits USVs

To determine whether the mPOA promotes USV production, we injected adeno-associated viruses (AAVs) encoding channelrhodopsin 2 (ChR2) or mCherry as the control, both driven by the human synapsin promoter (hSyn), unilaterally into the mPOA of adult virgin C57BL/6 mice, and implanted optical fibers (Fig. 1A) [43]. This strategy allowed us to optogenetically activate the mPOA while monitoring USV production with a recording system in a fresh cage (Fig. 1B). Phasic light stimulation (15 s, 12 mW, 40 Hz, 10-ms pulses) was randomly delivered. *Post-hoc* c-Fos analysis revealed that optogenetically-induced neuronal activation was mainly restricted to the mPOA [43]. Strikingly, we found that optogenetic activation of the mPOA reliably elicited the production of USVs in the absence of any social stimulus (Fig. 1C). Detailed analysis of the spectrogram revealed that optogenetically-activated USVs contained distinct units or syllables predominantly around 70 kHz, similar to courtship USVs (Fig. 1D) [7, 47]. In total, > 75% of ChR2-injected animals emitted USVs under light stimulation while none of the controls did (Fig. 1E). No sex differences were detected, consistent with our previous results showing that the mPOA can drive sexually dimorphic behaviors in both sexes [43]. The probability that a given light stimulation would elicit USVs

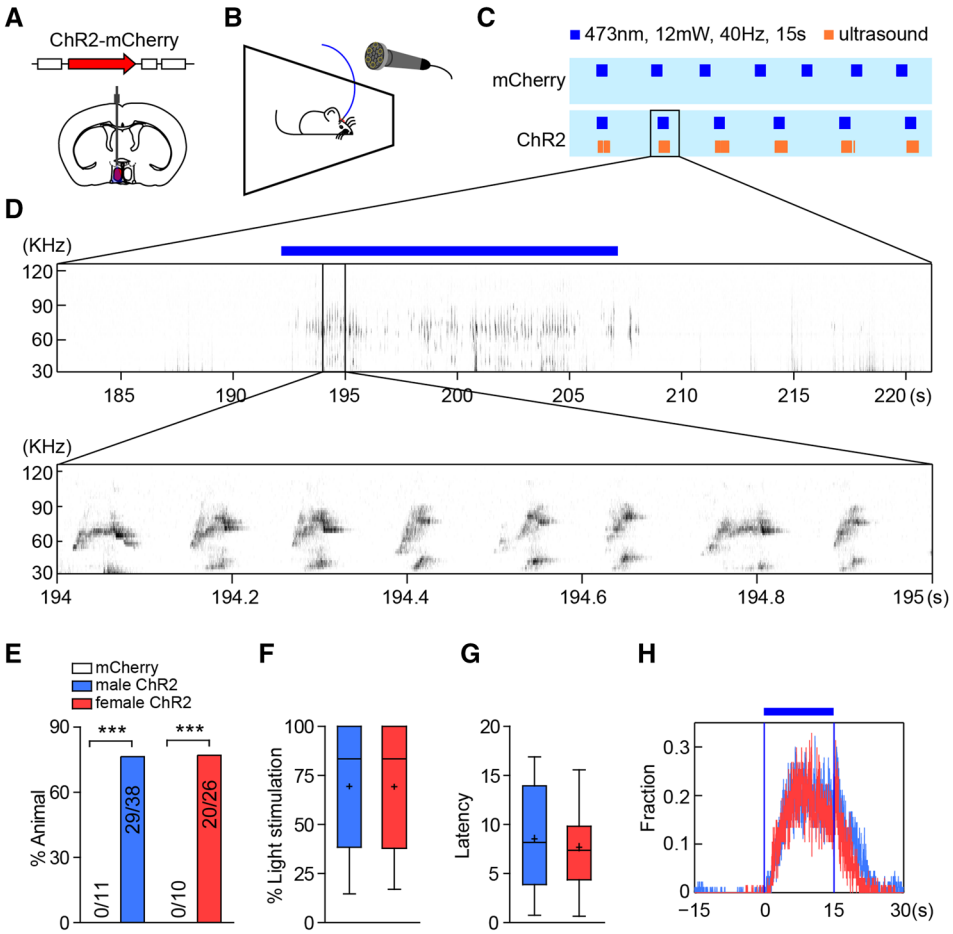

Fig. 1 Optogenetic activation of mPOA induces USVs. **A** Schematic of the strategy to optogenetically activate mPOA neurons in wild-type animals. **B** Schematic of the behavioral setup to optogenetically activate the mPOA while recording USVs. Animals were tested in a fresh mouse cage alone without any social stimulus. **C** Representative raster plots showing the emission of USVs (orange bars) in the ChR2 but not the mCherry group during periods of optogenetic activation (blue bars). **D** Upper panel, time-frequency-power display of USVs induced by a single period of light stimulation in the box highlighted in **C**. Lower panel, expanded view of the time-frequency-power display between the two lines in the upper panel to reveal individual syllables. **E** Percentages of animal that displayed optogenetically-induced USVs. **F–H** Probability of a USV being elicited by light (**F**), latency of USVs (**G**), and average distribution of optogenetically-induced USVs (**H**) (n = 11 mCherry and 38 ChR2 males, 10 mCherry and 26 ChR2 females. Fisher's exact test in **E**. $***P < 0.001$).

varied across animals with the success rate reaching 100% in some animals and a median of ~ 80% across all animals (Fig. 1F). The median latency for detection of USVs after the delivery of light was ~ 8 s but ranged from within 1 s to > 15 s (Fig. 1G). This inter-individual variability likely reflects variations in the surgery and viral expression, even though the target sites of all animals were confirmed to be within the mPOA as previously described [43]. Furthermore, the majority of the elicited USVs occurred within the stimulation period, with some tapering-off after termination of the stimulation (Fig. 1H). Taken together, these results explicitly demonstrate that activation of the mPOA is sufficient to drive USV production in both sexes.

Optogenetically-Induced USVs are Similar to Courtship USVs

To gain further insights into the biological meaning of optogenetically-activated USVs, we performed more detailed analysis of the syllable composition and spectral features of these USVs using Mouse Song Analyzer 1.3 as previously described [7, 11, 16, 45, 46] and compared them to courtship USVs emitted spontaneously by males towards a female stimulus. In total, 9 types were distinguished by the software (Fig. 2A). These included, for continuous syllables without pitch jumps: (1) a type with a duration < 5 ms defined as "short"; (2) a type with a constant frequency defined as "flat"; (3 and 4) types with a continuous increase or decrease in frequency defined as "upward (up)" or "downward (down)"; and (5) a type with

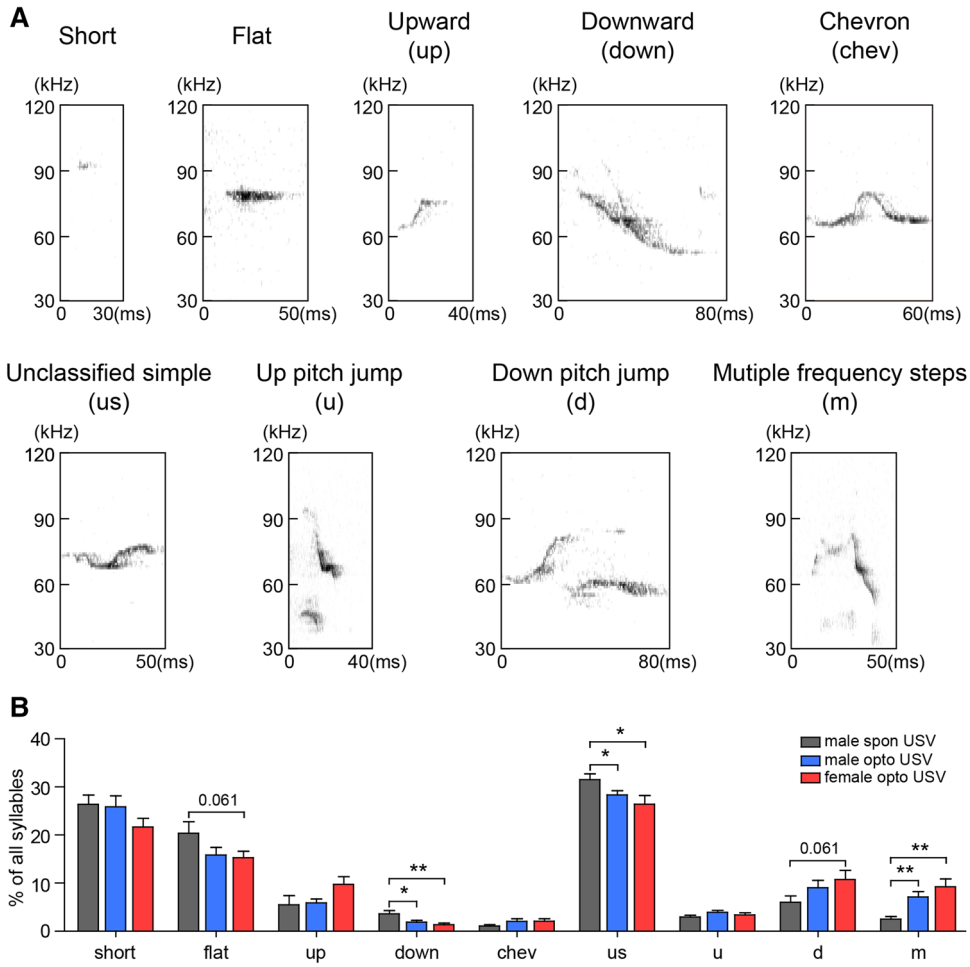

Fig. 2 Syllable types and composition of optogenetically-induced and spontaneously-emitted courtship USVs. **A** Representative time-frequency-power displays showing the major call types identified in optogenetically-induced USVs. **B** Syllable composition of optogenetically-induced and spontaneously-emitted courtship USVs. The percentage of each call type was first calculated for individual animals and then averaged across animals within each group (n = 13 male spontaneous (spon) USVs, 23 male optogenetic (opto) USVs, and 16 female opto USVs). $^{*}P < 0.05$, $^{**}P < 0.01$, unpaired t-test.

a continuous increase followed by a continuous decrease in frequency defined as "chevron (chev)". All other continuous syllables were defined as "unclassified simple (us)". Other defined types of syllables that contained instantaneous pitch jumps included "up pitch jump (u)", "down pitch jump (d)", and "multiple frequency steps (m)". Interestingly, while the composition of each syllable type in optogenetically-induced and spontaneously-emitted courtship USVs were similar, subtle but significant differences were detected in the usage of several syllable types (Fig. 2B). Specifically, there were fewer "flat", "down", and "us" types but more "d" and "m" types in optogenetically-induced USVs (Fig. 2B), suggesting greater complexity.

Next, we analyzed in detail the acoustic features of syllables identified in optogenetically-elicited and spontaneously-emitted USVs (Fig. 3A). The inter-syllable interval of optogenetically-induced USVs tracked closely with the spontaneously-emitted USVs, most syllables being emitted < 250 ms apart (Fig. 3B). Using a cutoff of 250 ms to segment sequences, we found that the average number of syllables within a given sequence was similar in the optogenetically-induced and spontaneously-emitted USVs (Fig. 3C). In addition, the average syllable duration and mean pitch frequency were also comparable in the optogenetically-induced and spontaneously-emitted USVs, while the bandwidth was wider and the spectral purity tended to be lower in optogenetically-induced USVs (Fig. 3D–G), again indicating increased complexity. As previous studies have shown that male mice emit more complex USVs during the later stages of mating than in the initial appetitive social interaction phase [47, 48], we separated out spontaneous USVs emitted during different stages of mating and compared them to optogenetically-induced USVs. Interestingly, in bandwidth and spectral purity, optogenetically-induced USVs were more similar to USVs emitted during mounting than those emitted during social interactions, while in syllable duration and mean pitch frequency, optogenetically-induced USVs appeared to be intermediate between the two (Fig. 3H–K). Taken together, these results show that optogenetically-elicited USVs are qualitatively similar to the courtship USVs emitted by males, especially those emitted during the consummation stage.

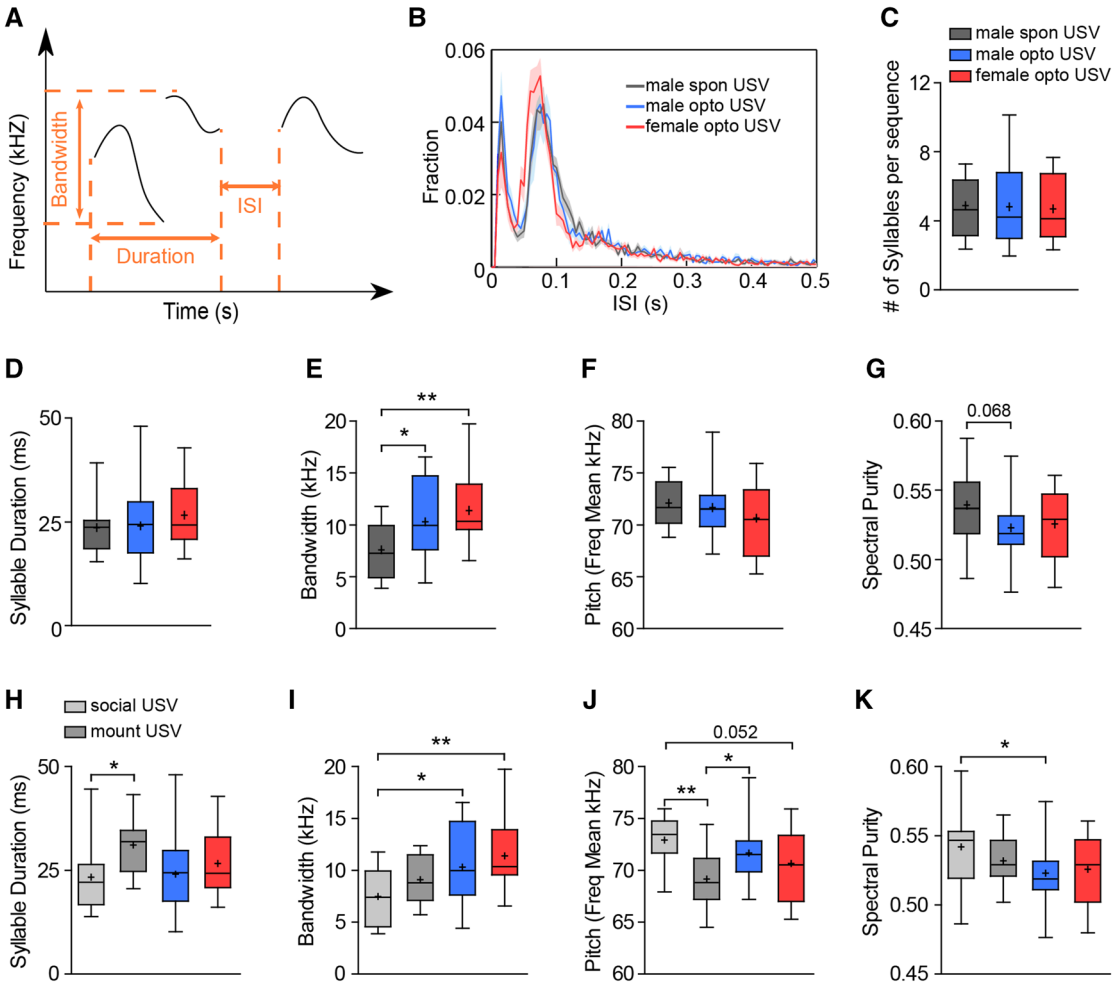

Fig. 3 Spectral features of optogenetically-induced USVs and courtship USVs. **A** Schematic of two syllables to show the spectral parameters analyzed for this figure. **B** Distribution of inter-syllable intervals (ISIs) of optogenetically-induced and spontaneously-emitted USVs. No differences were found. **C** Sequence length as measured by the average number of syllables per sequence with an ISI cutoff of 250 ms in spontaneously-emitted and optogenetically-induced USVs. **D–G** Average syllable duration (**D**), bandwidth (frequency range of syllables) (**E**), mean pitch frequency (**F**), and spectral purity (**G**) in optogenetically-induced and spontaneously-emitted courtship USVs. **H–K** Average syllable duration (**H**), bandwidth (**I**), mean pitch frequency (**J**), and spectral purity (**K**) in optogenetically-induced and spontaneously-emitted courtship USVs during the initial social interaction stage (social USV) and those emitted after mounting behaviors had been initiated (mount USV). All parameters were first calculated for each syllable and then averaged at the animal level and subsequently across animals in each group. $n = 13$ male spontaneous (spon) USVs (13 social USVs and 8 mounting USVs), 23 male optogenetic (opto) USVs, and 16 female opto USVs. $^{*}P < 0.05$, $^{**}P < 0.01$, unpaired *t*-test.

mPOA Vgat+ Neurons are Effective in Driving USV Production

To determine which population of mPOA neurons underlie USV production, we specifically targeted mPOA Vgat+ and Vglut2+ neurons using Cre driver lines that had already been generated [44, 49]. As shown previously, Vgat+ neurons make up ~ 80% of all NeuN +/HuCD+ cells in the mPOA and thus account for the majority of mPOA neurons [43]. We first validated the specificity and fidelity of these lines by unilaterally injecting AAVs encoding Cre-inducible EYFP into the mPOA of Vgat-Cre and Vglut2-Ires-Cre animals (Fig. 4A). *In situ* and immunohistochemical co-staining revealed that ~ 95% of EYFP-labeled neurons co-localized with *Vgat*+ and *Vglut2*+ cells (Fig. 4B) (Vgat-Cre, 94.66% ± 1.58%, $n = 2$ males and 2 females; Vglut2-Cre, 94.45% ± 0.36%, $n = 2$ males and 2 females), suggesting correct targeting. Next, we activated mPOA Vgat+ or Vglut2+ neurons by injecting AAVs encoding Cre-inducible ChR2, or mCherry as the control, unilaterally into the mPOA of Vgat-Cre or Vglut2-Ires-Cre mice, and implanting optical fibers (Fig. 4C). Mice were tested with the same protocol as mPOA pan-neuronal activation (Fig. 1B). In Vgat-Cre animals, 7 out of 7 male mice and 6 out of 10 female mice injected with ChR2 virus emitted

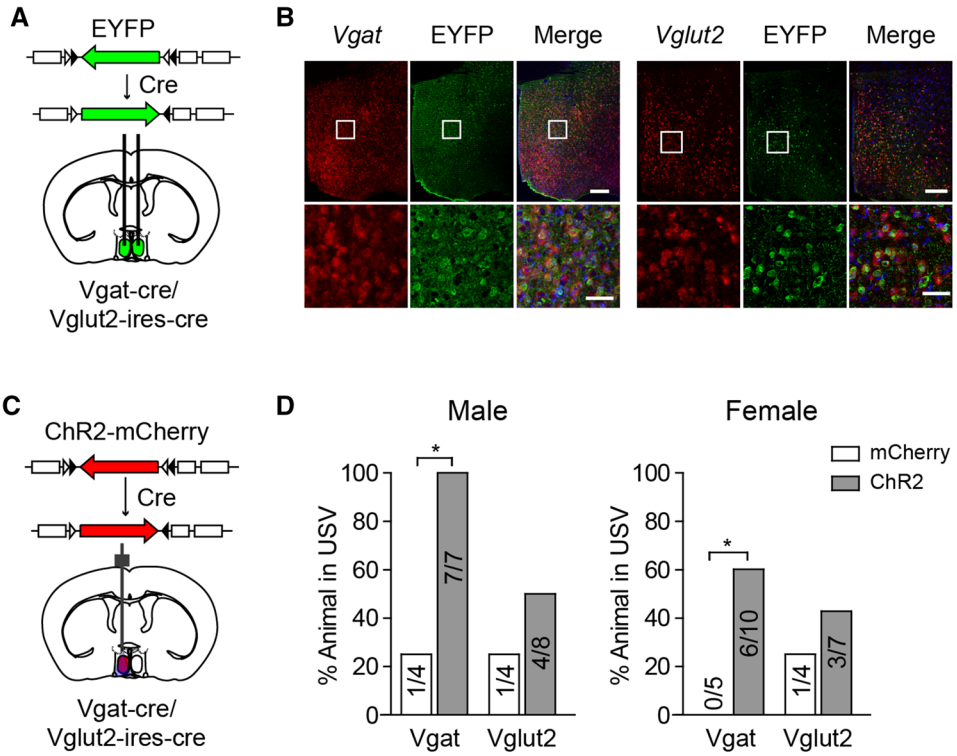

Fig. 4 mPOA Vgat+ neurons are effective at driving USV production. **A** Schematic showing the strategy to validate the specificity of Vgat-Cre and Vglut2-Ires-Cre lines by viral injection of Cre-inducible EYFP. **B** Representative images showing the co-localization of EYFP immunohistochemical signals with *Vgat* or *Vglut2* signals *in situ*. Lower panels, magnification of white boxes in upper panel. Scale bars, upper panels, 200 μm; lower panels, 50 μm. **C** Schematic showing the strategy to specifically activate mPOA Vgat+ or Vglut2+ neurons by viral injection of Cre-inducible ChR2. **D** Percentages of mice displaying optogenetically-induced USVs in Vgat-Cre and Vglut2-Cre mice injected with ChR2 or control mCherry virus. $*P < 0.05$, Fisher's exact test.

USVs during light stimulation; this was significantly higher than the control group (Fig. 4D). By comparison, 4 out of 8 Vglut2-Cre males and 3 out of 7 Vglut2-Cre females injected with ChR2 virus also displayed optogenetically-induced USVs (Fig. 4D); this was not significantly different from the control group and also appeared to be lower than Vgat-Cre animals. Similarly, the probability of light activating USVs in a given stimulation also tended to be higher for Vgat+ ChR2 animals (male, Vgat-Cre, 69.29% ± 15.47%; Vglut2-Ires-Cre, 35.27% ± 13.92%, unpaired *t*-test, $P = 0.18$; female, Vgat-Cre, 75% ± 13.44%; Vglut2-Ires-Cre, 27.78% ± 11.11%, unpaired *t*-test, $P = 0.06$). Thus, these optogenetic "gain-of-function" experiments demonstrate that activation of mPOA Vgat+ neurons is sufficient to elicit USV production in adult mice of both sexes in the absence of any social stimulus.

Ablation of mPOA Vgat+ Neurons Alters Spectral Features of Courtship USVs

Next, to test whether mPOA Vgat+ neurons indeed regulate USV production under physiological conditions, we performed loss-of-function experiments by injecting AAVs encoding Cre-inducible caspase3 bilaterally into the mPOA of Vgat-Cre animals of both sexes to specifically eliminate these neurons (Fig. 5A). Control animals were Vgat-Cre mice injected with AAVs encoding Cre-inducible mCherry and wild-type littermates injected with the same caspase3 virus. We previously showed that such an approach results in ~ 80% of Vgat+ neurons being eliminated as evidenced by the loss of *GAD1 in situ* signals in caspase3-injected animals compared to controls (Fig. 5B) [43]. For behavioral testing, each animal was exposed to a female intruder in its home cage for 5 min, during which time USVs were recorded. At the gross level, we did not find any deficit in USV production after ablation of mPOA Vgat+ neurons. The percentage of animals that emitted USVs, the latency, and the total duration of USVs remained the same in caspase3-injected animals as in controls (Fig. 5C–E). These results are consistent with a previous study showing that destruction of the mPOA does not affect the number of courtship USVs in males [50]. However, when we performed more detailed analysis of the acoustic features of USVs (only data points from males that displayed no mounting during the 5-min recording period were included for analysis), we found that ablation of mPOA Vgat+ neurons significantly increased the average syllable duration and bandwidth and significantly decreased the mean pitch frequency in caspase3-injected males but not females compared to the controls (Fig. 5F–H). By comparison, no differences were found in spectral purity or the number of syllables per sequence between caspase3 and control groups of either sex (Fig. 5I–J).

To investigate whether these changes in acoustic features are accompanied by alterations in syllable usage,

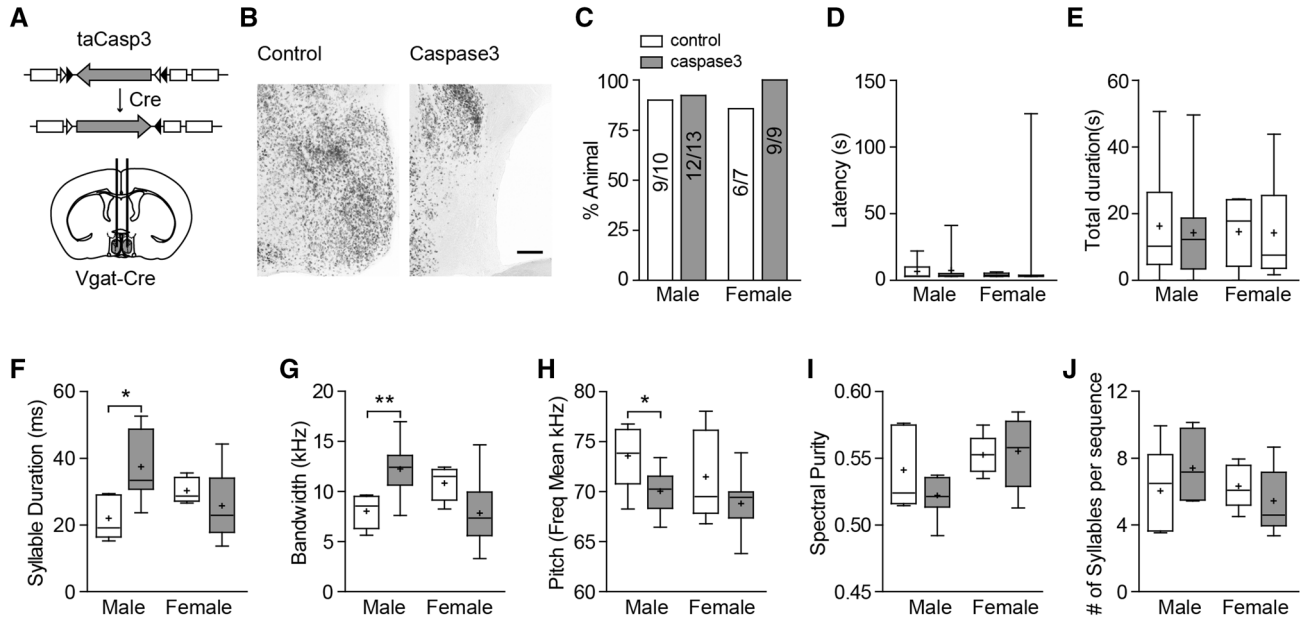

Fig. 5 Ablation of mPOA Vgat+ neurons alters distinct spectral features but not general numbers of USVs. **A** Schematic of the strategy to specifically ablate mPOA Vgat+ neurons by bilaterally injecting AAVs encoding Cre-inducible caspase3 (taCasp3) or mCherry as the control, into the mPOA of Vgat-Cre animals. **B** Example images of *GAD67 in situ* signals showing successful elimination of Vgat+ neurons in a caspase3-injected animal and a control. Scale bar, 200 µm. Group-level quantification of these images are provided in our previous study [43]. **C** Percentages of animals that emitted USVs during 5-min social interactions with a hormonally-primed ovariectomized (OVX) female intruder. Fisher's exact test, no differences detected. **D–E** Latency (**D**) and total duration (**E**) of USVs emitted during 5-min social interactions with a hormonally-primed OVX female. Two-way ANOVA followed by Bonferroni post-tests. No differences detected (n = 10 control and 13 caspase3 males and 7 control and 9 caspase3 females). Latency: virus effect, $F(1, 32) = 0.84$, $P = 0.3675$; sex effect, $F(1,32) = 0.19$, $P = 0.6694$; interaction effect, $F(1, 32) = 0.7$, $P = 0.4093$; total duration: virus effect, $F(1, 35) = 0.06$, $P = 0.8042$; sex effect, $F(1,35) = 0.03$, $P = 0.8583$; interaction effect, $F(1, 35) = 0.03$, $P = 0.8557$. **F–J** Spectral features of emitted USVs: syllable duration (**F**), bandwidth (**G**), pitch (**H**), spectral purity (**I**), and sequence length (**J**). Two-way ANOVA followed by Bonferroni post-tests (n = 5 control and 9 caspase3 males and 5 control and 9 caspase3 females). Duration, virus effect, $F(1, 24) = 2.45$, $P = 0.1308$; sex effect, $F(1,24) = 2.58$, $P = 0.24$; interaction effect, $F(1, 24) = 7.97$, $P = 0.0094$; bandwidth: virus effect, $F(1, 24) = 0.35$, $P = 0.5622$; sex effect, $F(1,24) = 0.57$, $P = 0.4563$; interaction effect, $F(1, 24) = 11.52$, $P = 0.0024$; pitch: virus effect, $F(1, 24) = 6.37$, $P = 0.0186$; sex effect, $F(1,24) = 1.87$, $P = 0.1843$; interaction effect, $F(1, 24) = 0.12$, $P = 0.7348$; spectral purity: virus effect, $F(1, 24) = 0.82$, $P = 0.3731$; sex effect, $F(1,24) = 6.34$, $P = 0.0189$; interaction effect, $F(1, 24) = 1.51$, $P = 0.2306$; number (#) of syllables per sequence: virus effect, $F(1, 24) = 0.10$, $P = 0.7545$; sex effect, $F(1,24) = 1.17$, $P = 0.2900$; interaction effect, $F(1, 24) = 2.07$, $P = 0.1630$. $^*P < 0.05$.

we compared the syllable composition of USVs emitted by caspase3 and control animals. Interestingly, we found male-specific changes in syllable usage, including significant increases in "down", "chev", and "m" types but also a decrease in "short" and "flat" types (Fig. 6A, upper panel). No such differences were found in female caspase3 animals (Fig. 6A, lower panel). Furthermore, when we restricted our analysis to syllable types that remained similarly used by caspase3 and control animals, the differences in acoustic features, including bandwidth and pitch frequency, disappeared (Fig. 6B), indicating that these changes are largely due to alterations in syllable composition. By contrast, the increase in syllable duration was still present (Fig. 6B). Taken together, these results demonstrate that the mPOA plays a male-specific role in modulating USV production, particularly syllable usage.

Discussion

In this study, we provided the first experimental evidence that optogenetic activation of a specific brain area, the mPOA, can elicit USVs that are similar to courtship USVs emitted by males towards females. While hormonal treatment has been shown to restore a male's ability to generate USVs towards females after castration [51, 52], in our experiments optogenetic activation of the mPOA was able to drive USV production in the absence of any social stimuli. Furthermore, we demonstrated that ablation of mPOA Vgat+ neurons led to male-specific changes in syllable usage and the acoustic features of courtship USVs.

The mPOA is a key node in a conserved neural network that controls social behaviors and is activated during social interactions [43, 53–56]. Therefore, it is well-positioned to detect female cues and drive USV production. Consistent with this idea, optogenetic activation of the mPOA in the

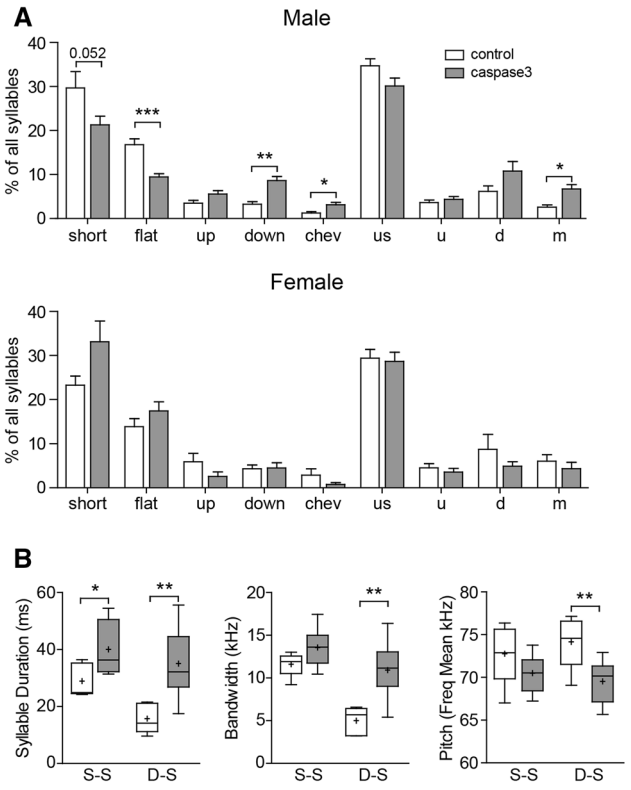

Fig. 6 Ablation of mPOA Vgat+ neurons changes syllable composition of emitted USVs in a male-specific manner. **A** Percentages of each type of syllable emitted by males (upper panel) and females (lower panel) during a 5-min social interaction with a hormonally-primed OVX female. Only data from videos in which no mounting occurred were included. The percentage was first calculated at an individual animal level and then averaged across animals within each group. Unpaired *t*-test. **B** The acoustic features "syllable duration", "bandwidth", and "pitch" analyzed separately among syllables used similarly in the caspase3 and control groups (similar syllable, S-S) and those used differently (D-S). $*P < 0.05$, $**P < 0.01$.

absence of social cues elicited USVs. Yet, previous results have shown that destruction of the mPOA, while dramatically reducing male sexual behaviors, leaves appetitive social interactions and behaviors including USVs mostly intact [43, 50]. Similarly, we found that ablation of mPOA Vgat+ neurons, the major neuronal population in the mPOA, though dramatically decreasing male mating behaviors, did not affect the levels of USVs emitted by the targeted (lesioned) mice toward a female intruder, indicating that the mPOA is dispensable for courtship USV production at the gross level. What then is the physiological role of the mPOA in USV production under normal conditions?

We propose that the mPOA plays a prominent role in modulating USV production to mediate context-dependent alterations in courtship USV content. For example, it is known that male mice emit USVs with a distinct composition and increased complexity during the later stages of mating compared to the initial appetitive phase [47, 48]. It can be imagined that the neural activity in the mPOA essential for the later stages of mating behaviors could in parallel modify USVs [43]. Indeed, with more detailed analysis, we showed that optogenetically-elicited USVs matched better with USVs emitted during the later stage of mating, in terms of bandwidth and spectral purity, and that ablation of mPOA Vgat+ neurons resulted in male-specific changes in syllable usage and acoustic features such as bandwidth, syllable duration, and pitch, demonstrating a modulatory role of the mPOA in courtship USVs. However, it remains unclear why both mPOA activation and ablation resulted in some similar changes in USV acoustic features and syllable composition, indicating nonlinearity in the system. As chronic and unintended damage to nearby regions is inherent in lesion studies [43], future optogenetic inhibition experiments that afford better temporal resolution than lesion experiments will more clearly resolve and reveal context- and stage-specific functions of the mPOA in courtship USV production.

In addition, female mice also emit USVs under various social conditions such as in response to other female intruders [13], during courtship chase [15], or during interactions with male mates in the context of parental care (mainly ~ 38 kHz) [57]. The very limited studies that have compared USVs emitted by females or males towards a female intruder have reported little difference [14]. However, it is not clear whether the semantic meanings or prosody may differ between USVs emitted by females and males. In our study, we found that optogenetic activation of the mPOA drove USV production in females similar to males in the absence of social stimuli, with all acoustic parameters analyzed comparable between the sexes. However, lesioning the mPOA seemed not to affect the numbers or acoustic features of USVs emitted by females towards a female intruder, further supporting a male-specific physiological function of the mPOA in modulating USVs. It will be interesting to determine whether the mPOA still plays a role in modulating USV production in females under other social conditions.

More importantly, our results on the mPOA provide an entry point to begin to dissect the neural circuits that underlie USV production in mice. What then might be other brain regions that critically regulate this process? One such candidate is the periaqueductal gray area (PAG) in the midbrain, a major downstream target of mPOA neurons outside the hypothalamus [58]. It is known that the PAG projects to pontine and medullary regions that are thought to contain premotor central pattern generator neurons important for respiration and vocalization [59]. Furthermore, bilateral lesions of the PAG lead to mutism [60]. Importantly, a recent study using an "activity tagging strategy" identified a subset of PAG neurons in males that are selectively activated during courtship USV production

[61]. Moreover, silencing these PAG neurons renders males mute and less attractive to females without affecting other components of courtship [61], demonstrating that the PAG constitutes an obligatory hub in the neural network that controls USV production. Thus, all regions upstream of PAG-USV neurons, which likely include the mPOA Vgat+ neurons and possibly other brain areas such as the anterior hypothalamus, the ventral medial hypothalamus, and the septum, could all play a role in driving or modifying USVs. Such a layout shares similarities with the vocal production systems in songbirds and humans [16, 42, 62], further supporting the notion that the mouse may also be a valuable additional organism in which to model and study the neural control of vocal production. In summary, our results lay a first step for such efforts to systematically dissect the neural mechanisms that govern USV production in mice.

Acknowledgements We thank members of the Xu's lab for comments on this manuscript, and Dr. Hai-Lan Hu's lab for help with USV equipment. This work was supported by grants from the National Natural Science Foundation of China (31871066, 31471065), the National Basic Research Development Program (973 Program) of China (2015CB559201), the Thousand Young Talents Program of China, the Strategic Priority Research Program of the Chinese Academy of Sciences (XDB32010200), and as part of the Chinese Academy of Science interdisciplinary innovation team.

Conflict of interest The authors claim no conflict of interest.

References

1. Egnor SR, Seagraves KM. The contribution of ultrasonic vocalizations to mouse courtship. Curr Opin Neurobiol 2016, 38: 1–5.
2. Heckman J, McGuinness B, Celikel T, Englitz B. Determinants of the mouse ultrasonic vocal structure and repertoire. Neurosci Biobehav Rev 2016, 65: 313–325.
3. Portfors CV, Perkel DJ. The role of ultrasonic vocalizations in mouse communication. Curr Opin Neurobiol 2014, 28: 115–120.
4. Nyby J, Wysocki CJ, Whitney G, Dizinno G. Pheromonal regulation of male mouse ultrasonic courtship (*Mus musculus*). Anim Behav 1977, 25: 333–341.
5. Whitney G, Coble JR, Stockton MD, Tilson EF. Ultrasonic emissions: do they facilitate courtship of mice. J Comp Physiol Psychol 1973, 84: 445–452.
6. Bean NJ. Olfactory and vomeronasal mediation of ultrasonic vocalizations in male mice. Physiol Behav 1982, 28: 31–37.
7. Holy TE, Guo Z. Ultrasonic songs of male mice. PLoS Biol 2005, 3: e386.
8. Pomerantz SM, Nunez AA, Bean NJ. Female behavior is affected by male ultrasonic vocalizations in house mice. Physiol Behav 1983, 31: 91–96.
9. Shepard KN, Liu RC. Experience restores innate female preference for male ultrasonic vocalizations. Genes Brain Behav 2011, 10: 28–34.
10. Hammerschmidt K, Radyushkin K, Ehrenreich H, Fischer J. Female mice respond to male ultrasonic 'songs' with approach behaviour. Biol Lett 2009, 5: 589–592.
11. Chabout J, Sarkar A, Dunson DB, Jarvis ED. Male mice song syntax depends on social contexts and influences female preferences. Front Behav Neurosci 2015, 9: 76.
12. Asaba A, Osakada T, Touhara K, Kato M, Mogi K, Kikusui T. Male mice ultrasonic vocalizations enhance female sexual approach and hypothalamic kisspeptin neuron activity. Horm Behav 2017, 94: 53–60.
13. Maggio JC, Whitney G. Ultrasonic vocalizing by adult female mice (Mus musculus). J Comp Psychol 1985, 99: 420–436.
14. Hammerschmidt K, Radyushkin K, Ehrenreich H, Fischer J. The structure and usage of female and male mouse ultrasonic vocalizations reveal only minor differences. PLoS One 2012, 7: e41133.
15. Neunuebel JP, Taylor AL, Arthur BJ, Egnor SE. Female mice ultrasonically interact with males during courtship displays. Elife 2015, 4. https://doi.org/10.7554/eLife.06203.
16. Arriaga G, Zhou EP, Jarvis ED. Of mice, birds, and men: the mouse ultrasonic song system has some features similar to humans and song-learning birds. PLoS One 2012, 7: e46610.
17. Hammerschmidt K, Reisinger E, Westekemper K, Ehrenreich L, Strenzke N, Fischer J. Mice do not require auditory input for the normal development of their ultrasonic vocalizations. BMC Neurosci 2012, 13: 40.
18. Mahrt EJ, Perkel DJ, Tong L, Rubel EW, Portfors CV. Engineered deafness reveals that mouse courtship vocalizations do not require auditory experience. J Neurosci 2013, 33: 5573–5583.
19. Scattoni ML, Gandhy SU, Ricceri L, Crawley JN. Unusual repertoire of vocalizations in the BTBR T + tf/J mouse model of autism. PLoS One 2008, 3: e3067.
20. Zampieri BL, Fernandez F, Pearson JN, Stasko MR, Costa AC. Ultrasonic vocalizations during male-female interaction in the mouse model of Down syndrome Ts65Dn. Physiol Behav 2014, 128: 119–125.
21. Choi H, Park S, Kim D. Two genetic loci control syllable sequences of ultrasonic courtship vocalizations in inbred mice. BMC Neurosci 2011, 12: 104.
22. Wang H, Liang S, Burgdorf J, Wess J, Yeomans J. Ultrasonic vocalizations induced by sex and amphetamine in M2, M4, M5 muscarinic and D2 dopamine receptor knockout mice. PLoS One 2008, 3: e1893.
23. Jiang YH, Pan Y, Zhu L, Landa L, Yoo J, Spencer C, *et al.* Altered ultrasonic vocalization and impaired learning and memory in Angelman syndrome mouse model with a large maternal deletion from *Ube3a* to *Gabrb3*. PLoS One 2010, 5: e12278.
24. Sugimoto H, Okabe S, Kato M, Koshida N, Shiroishi T, Mogi K, *et al.* A role for strain differences in waveforms of ultrasonic vocalizations during male-female interaction. PLoS One 2011, 6: e22093.
25. Panksepp JB, Jochman KA, Kim JU, Koy JJ, Wilson ED, Chen Q, *et al.* Affiliative behavior, ultrasonic communication and social reward are influenced by genetic variation in adolescent mice. PLoS One 2007, 2: e351.
26. Gaub S, Fisher SE, Ehret G. Ultrasonic vocalizations of adult male Foxp2-mutant mice: behavioral contexts of arousal and emotion. Genes Brain Behav 2016, 15: 243–259.
27. Wohr M. Ultrasonic vocalizations in Shank mouse models for autism spectrum disorders: detailed spectrographic analyses and developmental profiles. Neurosci Biobehav Rev 2014, 43: 199–212.
28. Castellucci GA, McGinley MJ, McCormick DA. Knockout of Foxp2 disrupts vocal development in mice. Sci Rep 2016, 6: 23305.
29. Ju A, Hammerschmidt K, Tantra M, Krueger D, Brose N, Ehrenreich H. Juvenile manifestation of ultrasound communication deficits in the neuroligin-4 null mutant mouse model of autism. Behav Brain Res 2014, 270: 159–164.

30. Chabout J, Sarkar A, Patel SR, Radden T, Dunson DB, Fisher SE, *et al*. A Foxp2 mutation implicated in human speech deficits alters sequencing of ultrasonic vocalizations in adult male mice. Front Behav Neurosci 2016, 10: 197.
31. Yu X, Qiu Z, Zhang D. Recent research progress in autism spectrum disorder. Neurosci Bull 2017, 33: 125–129.
32. Masi A, DeMayo MM, Glozier N, Guastella AJ. An overview of autism spectrum disorder, heterogeneity and treatment options. Neurosci Bull 2017, 33: 183–193.
33. Scattoni ML, Crawley J, Ricceri L. Ultrasonic vocalizations: a tool for behavioural phenotyping of mouse models of neurodevelopmental disorders. Neurosci Biobehav Rev 2009, 33: 508–515.
34. Zala SM, Reitschmidt D, Noll A, Balazs P, Penn DJ. Sex-dependent modulation of ultrasonic vocalizations in house mice (*Mus musculus musculus*). PLoS One 2017, 12: e0188647.
35. Grimsley JM, Sheth S, Vallabh N, Grimsley CA, Bhattal J, Latsko M, *et al*. Contextual modulation of vocal behavior in mouse: newly identified 12 kHz "mid-frequency" vocalization emitted during restraint. Front Behav Neurosci 2016, 10: 38.
36. Hoier S, Pfeifle C, von Merten S, Linnenbrink M. Communication at the garden fence–context dependent vocalization in female house mice. PLoS One 2016, 11: e0152255.
37. Yang M, Loureiro D, Kalikhman D, Crawley JN. Male mice emit distinct ultrasonic vocalizations when the female leaves the social interaction arena. Front Behav Neurosci 2013, 7: 159.
38. Scattoni ML, Ricceri L, Crawley JN. Unusual repertoire of vocalizations in adult BTBR T + tf/J mice during three types of social encounters. Genes Brain Behav 2011, 10: 44–56.
39. D'Amato FR, Moles A. Ultrasonic vocalizations as an index of social memory in female mice. Behav Neurosci 2001, 115: 834–840.
40. Nyby J, Dizinno GA, Whitney G. Social status and ultrasonic vocalizations of male mice. Behav Biol 1976, 18: 285–289.
41. Holfoth DP, Neilans EG, Dent ML. Discrimination of partial from whole ultrasonic vocalizations using a go/no-go task in mice. J Acoust Soc Am 2014, 136: 3401–3409.
42. Arriaga G, Jarvis ED. Mouse vocal communication system: are ultrasounds learned or innate? Brain Lang 2013, 124: 96–116.
43. Wei YC, Wang SR, Jiao ZL, Zhang W, Lin JK, Li XY, *et al*. Medial preoptic area in mice is capable of mediating sexually dimorphic behaviors regardless of gender. Nat Commun 2018, 9: 279.
44. Chao HT, Chen H, Samaco RC, Xue M, Chahrour M, Yoo J, *et al*. Dysfunction in GABA signalling mediates autism-like stereotypies and Rett syndrome phenotypes. Nature 2010, 468: 263–269.
45. Chabout J, Jones-Macopson J, Jarvis ED. Eliciting and analyzing male mouse ultrasonic vocalization (USV) songs. J Vis Exp 2017, 123: 54137. https://doi.org/10.3791/54137.
46. Weiner B, Hertz S, Perets N, London M. Social ultrasonic vocalization in awake head-restrained mouse. Front Behav Neurosci 2016, 10: 236.
47. White NR, Prasad M, Barfield RJ, Nyby JG. 40- and 70-kHz vocalizations of mice (*Mus musculus*) during copulation. Physiol Behav 1998, 63: 467–473.
48. Matsumoto YK, Okanoya K. Phase-specific vocalizations of male mice at the initial encounter during the courtship sequence. PLoS One 2016, 11: e0147102.
49. Vong L, Ye C, Yang Z, Choi B, Chua S Jr, Lowell BB. Leptin action on GABAergic neurons prevents obesity and reduces inhibitory tone to POMC neurons. Neuron 2011, 71: 142–154.
50. Bean NY, Nunez AA, Conner R. Effects of medial preoptic lesions on male mouse ultrasonic vocalizations and copulatory behavior. Brain Res Bull 1981, 6: 109–112.
51. Matochik JA, Sipos ML, Nyby JG, Barfield RJ. Intracranial androgenic activation of male-typical behaviors in house mice: motivation versus performance. Behav Brain Res 1994, 60: 141–149.
52. Sipos ML, Nyby JG. Concurrent androgenic stimulation of the ventral tegmental area and medial preoptic area: synergistic effects on male-typical reproductive behaviors in house mice. Brain Res 1996, 729: 29–44.
53. Han Y, Li XY, Wang SR, Wei YC, Xu XH. Presence of pups suppresses hunger-induced feeding in virgin adult mice of both sexes. Neuroscience 2017, 362: 228–238.
54. Zha X, Xu X. Dissecting the hypothalamic pathways that underlie innate behaviors. Neurosci Bull 2015, 31: 629–648.
55. Newman SW. The medial extended amygdala in male reproductive behavior. A node in the mammalian social behavior network. Ann N Y Acad Sci 1999, 877: 242–257.
56. O'Connell LA, Hofmann HA. Evolution of a vertebrate social decision-making network. Science 2012, 336: 1154–1157.
57. Liu HX, Lopatina O, Higashida C, Fujimoto H, Akther S, Inzhutova A, *et al*. Displays of paternal mouse pup retrieval following communicative interaction with maternal mates. Nat Commun 2013, 4: 1346.
58. Kohl J, Babayan BM, Rubinstein ND, Autry AE, Marin-Rodriguez B, Kapoor V, *et al*. Functional circuit architecture underlying parental behaviour. Nature 2018, 556: 326–331.
59. Menuet C, Cazals Y, Gestreau C, Borghgraef P, Gielis L, Dutschmann M, *et al*. Age-related impairment of ultrasonic vocalization in Tau.P301L mice: possible implication for progressive language disorders. PLoS One 2011, 6: e25770.
60. Esposito A, Demeurisse G, Alberti B, Fabbro F. Complete mutism after midbrain periaqueductal gray lesion. Neuroreport 1999, 10: 681–685.
61. Tschida K, Michael V, Han BX, ZHao Sl, Sakurai K, Mooney R, *et al*. Identification of midbrain neurons essential for vocal communication. BioRxiv 2018.
62. Petkov CI, Jarvis ED. Birds, primates, and spoken language origins: behavioral phenotypes and neurobiological substrates. Front Evol Neurosci 2012, 4: 12.